Scaling the energy conversion rate from magnetic field reconnection to different bodies

F. S. Mozer and A. Hull
Space Sciences Laboratory, University of California, Berkeley, California 94720, USA

(Received 25 June 2010; accepted 28 September 2010; published online 29 October 2010)

Magnetic field reconnection is often invoked to explain electromagnetic energy conversion in planetary magnetospheres, stellar coronae, and other astrophysical objects. Because of the huge dynamic range of magnetic fields in these bodies, it is important to understand energy conversion as a function of magnetic field strength and related parameters. It is conjectured theoretically and shown experimentally that the energy conversion rate per unit area in reconnection scales as the cube of an appropriately weighted magnetic field strength divided by the square root of an appropriately weighted density. With this functional dependence, the energy release in flares on the Sun, the large and rapid variation of the magnetic flux in the tail of Mercury, and the apparent absence of reconnection on Jupiter and Saturn, may be understood. Electric fields at the perihelion of the Solar Probe Plus mission may be tens of V/m. © *2010 American Institute of Physics*. [doi:10.1063/1.3504224]

I. INTRODUCTION

Magnetic field reconnection occurs when two magnetized plasmas, having a sheared magnetic field across their interface, flow toward each other.[1] Its characteristic feature is a modification of the original magnetic field topology that results from the presence in some relatively small region of dissipative processes that convert electromagnetic energy to plasma energy.[2,3] A plasma from one of the inflowing regions becomes magnetically connected to another plasma from the other inflowing region as a result of the topological change due to reconnection. The magnetic field geometry of reconnection is illustrated in Fig. 1, in which a thin sheet of current (the rectangle of Fig. 1), flowing into the plane of the figure (in the +Y-direction), is associated with the shear in the magnetic field component B_Z. The X-direction is normal to the thin current sheet and the Z-direction is that of the reconnecting magnetic field components that combine to form the reconnected magnetic field lines above and below the X-line, at the center of the figure.

Magnetic field reconnection may be invoked to explain cosmic rays with energies as great as 10^{20} eV (Ref. 4) as well as the 18-order-of-magnitude range of energy release between laboratory machines, the terrestrial magnetosphere, the Sun, the galactic diffuse x-ray emission, the radio lobes, and the Crab Nebula.[4,5] To understand this tremendous dynamic range, it is necessary to know the dependence of a single reconnection event on the magnetic field strength and associated parameters. In Sec. II, it is conjectured that the energy conversion rate per unit area in a single reconnection event scales as the cube of an appropriately weighted average magnetic field strength divided by the square root of an appropriately weighted density. In Sec. III, it is conjectured that $E_X = B_1(B_1+B_2)/80.38\ dn_0^{0.5}$, where B_1 and B_2 are the reconnecting magnetic fields on the two sides of the current sheet, n_0 is a weighted plasma density, and d is the current sheet thickness in units of the ion skin depth. In Sec. IV, the Polar satellite observations of subsolar reconnection, occurring over a factor of 10 in magnetic field strengths, are analyzed to show that this functional form for E_X provides a better fit to the experimental data than do modified functions of B and n_0, and that R^2, the fraction of the total squared error explained by this functional form, is a surprisingly large 0.90. Section V utilizes the scaling relationships to discuss reconnection in the solar system and to show that on the Sun, a single reconnection event occurring over a reasonable area may release enough energy to explain solar flares; at Mercury, it may account for flux pileup in the tail; and at Jupiter and Saturn, reconnection is probably negligible. Section VI briefly comments on scaling in the astrophysical context.

II. CONJECTURE THAT E_Y SCALES AS $B_0^2/n_0^{0.5}$ AND THAT THE ENERGY CONVERSION RATE SCALES AS $B_0^3/n_0^{0.5}$

In the following discussion, it is initially assumed that the reconnection geometry is two dimensional, that the plasma densities and the magnitudes of B_Z at the right and left sides of Fig. 1 are the same, and that $B_Y=0$. In the presence of an into-the-plane electric field ($E_Y>0$), the plasma flows toward the center of the figure from each side at the velocity of $\mathbf{E}\times\mathbf{B}/B^2=E_Y/B_Z$. This speed may be normalized by the Alfvén speed, $V_A=[B^2/\mu_0\ mn]^{0.5}$, where m is the ion mass, to form the dimensionless reconnection rate defined as

$$\text{Reconnection rate} \equiv E_Y/(B_Z V_A). \tag{1}$$

In many simulations[6] and measurements,[7,8] this reconnection rate is constant within a factor of 2 or so at a value of ~0.1. In accordance with such results, we assume that the reconnection rate is constant at the value M=0.1 in all reconnecting plasmas. In this case, Eq. (1) becomes

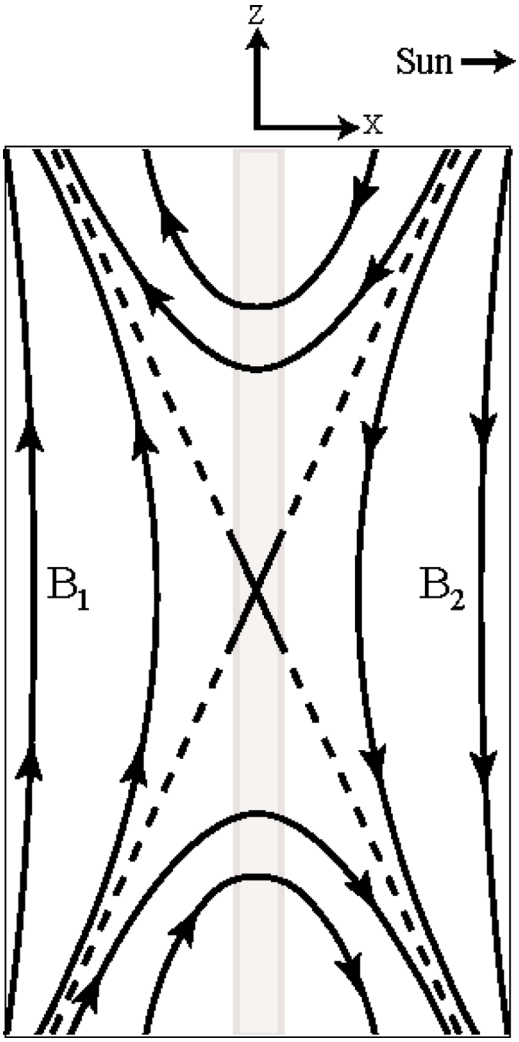

FIG. 1. (Color online) The magnetic field geometry for reconnection resulting from two plasmas flowing toward each other with a sheared magnetic field at their interface.

$$E_Y = MV_A B_Z \ \alpha \ B_z^2/n^{0.5}. \quad (2)$$

This dependence has also been found in computer simulations.[9]

The magnetic flux that reconnects per second per unit length is the field line inflow speed, $\mathbf{E}\times\mathbf{B}/B^2$, times the density of field lines, B, which, for the present case, simplifies to being E_Y. Thus, the flux reconnection rate is proportional to $B_Z^2/n^{0.5}$, which is more than 10^7 times greater in the solar corona than at the Earth's subsolar magnetopause, in spite of the fact that the reconnection rate, defined by Eq. (1), is the same at the two locations if M=0.1.

To make quantitative comparisons of the measured and expected electric fields in asymmetric reconnection, it is necessary to modify Eq. (2) to accommodate the more general case of different plasma densities and reconnecting magnetic field magnitudes at the two sides of the reconnection region. In this case,[10,11] B_Z, n, and V_A are replaced by

$$B_0 = 2B_1B_2/(B_1 + B_2),$$

$$n_0 = (n_1B_2 + n_2B_1)/(B_1 + B_2),$$

and

$$V_0 = [B_1B_2/\mu_0\, mn_0]^{0.5},$$

where B_1 and B_2 are the absolute values of the reconnecting magnetic field strengths on the two sides of the current sheet, as illustrated in Fig. 1, and n_1 and n_2 are the plasma densities on the two sides. Thus, Eq. (2) for asymmetric reconnection becomes

$$E_Y = MV_0B_0 \ \alpha \ B_0(B_1B_2)^{0.5}/n_0^{0.5}. \quad (3)$$

This is the quantitative expression for E_Y that will be used for making the first comparisons ever made with experimental data in the terrestrial magnetosphere.

Because the energy conversion rate per unit area is proportional to the Poynting vector, $\mathbf{E}\times\mathbf{B}/\mu_0$, entering on each side of the current sheet,

$$\text{Energy conversion rate per unit area } \alpha \ MV_0B_0(B_1 + B_2)/\mu_0. \quad (4a)$$

For scaling to other objects where the reconnection magnetic fields and plasma densities on the two sides of the current sheet are not known, the dependences on these parameters will be ignored and the general scaling law that will be invoked is

$$\text{energy conversion rate per unit area } \alpha \ B^3/n^{0.5}. \quad (4b)$$

III. CONJECTURE THAT E_X IS PROPORTIONAL TO $B_1(B_1+B_2)/n_0^{0.5}$

The generalized Ohm's law is

$$\mathbf{E} + \mathbf{U}_I \times \mathbf{B} = \mathbf{j}\times\mathbf{B}/en - \nabla\cdot\mathbf{P}_e/en - (m_e/e)[\partial\mathbf{U}_e/\partial t + (\mathbf{U}_e\bullet\nabla)\mathbf{U}_e] + \eta\mathbf{j}, \quad (5)$$

where $\mathbf{U}_I$ is the ion flow speed, $\nabla\cdot\mathbf{P}_e$ is the divergence of the electron pressure tensor, and η is the resistivity. In the ion diffusion region of a collisionless reconnection event, the ion flow is small, and the second, third, fourth, and fifth terms on the right are negligible.[12] In this case,

$$E_X = j_Y B_Z/en. \quad (6)$$

The out-of-plane current j_Y is given by Ampere's law as $(B_1+B_2)/\mu_0\delta$, where δ is the thickness of the current sheet in the X-direction. Expressing δ in units of the ion skin depth, $c/\omega_{pI}=c(ne^2/\varepsilon_0 m)^{-0.5}$ gives

$$d = \delta/(c/\omega_{pI}). \quad (7)$$

The quantity d is conjectured to be independent of magnetic field and density, both because numerous simulations[12] and observations[13] have shown that reconnection commences and is strongest when the current sheet thins to dimensions of the order of the ion skin depth and also because the quality of the least-squares fits to experimental data that will be discussed below serve to validate this conjecture. B_Z in Eq. (6) is also assumed to be 0.5 B_1 because the large E_X value is found on the magnetospheric side of the magnetopause at a location where the magnetic field is about half of the peak

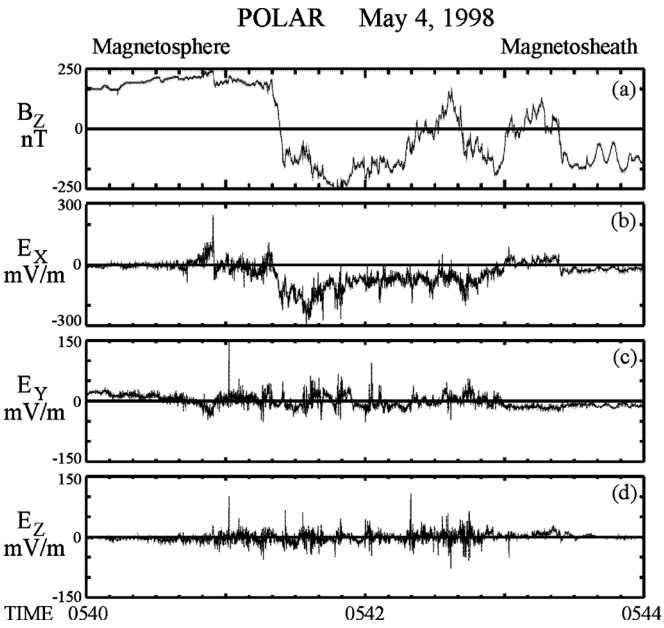

FIG. 2. Electric fields in mV/m and magnetic fields in nanotesla obtained on the Polar satellite during a 4 min interval in which the magnetopause was crossed at 1040 magnetic local time and 14° magnetic latitude. The data have been rotated into the minimum variance coordinate system. Note that the amplitude scales for E_Y and E_Z in panels (c) and (d) differ by a factor of 2 from that for E_X in panel (b). The magnetosphere is at the left of the figure with its positive B_Z in panel (a), and the magnetosheath, on the right, has a negative reconnection magnetic field.

value.[14] The density n appearing in both Eq. (6) and the ion skin depth is found empirically to be intermediate between the densities on the two sides of the current sheet at the time of the peak value of E_X.[14] So, it is replaced by the quantity n_0, which is both a density, which is intermediate between the densities on the two sides, and the appropriate expression when the asymmetries are not large. With these assumptions and with E_X in mV/m, n_0 in cm^{-3}, and B in nanotesla, Eq. (6) becomes

$$E_X = B_1(B_1 + B_2)/(80.38\ \ dn_0^{0.5}). \tag{8}$$

This is the quantitative expression for E_X that will be used for the first time to compare with experimental data in the terrestrial magnetosphere.

IV. EXPERIMENTAL DATA

Equations (3) and (8) for E_Y and E_X, respectively, have been tested against Polar satellite data, an example of which, in Fig. 2, shows a subsolar magnetopause crossing at a geocentric distance of 5.3 Earth radii, which is the closest magnetopause event to the Earth recorded in the 13 year Polar mission. Because the dipole magnetic field of the Earth varies inversely as the cube of the radial distance, the expected magnetospheric magnetic field should be about $(9/5.3)^3 \sim 5$ times larger than the typical 50 nT field observed for reconnection at the typical 9 Earth radius event distance observed on Polar. As shown in panel (a), the observed reconnection field agrees with this extrapolation, having an average value of 230 nT in the magnetosphere, to the left of Figs. 1 and 2. The average field in the magnetosheath during the final 30 s of Fig. 2 is −161 nT.

For plasma densities of 7 and 16 cm^{-3} in the magnetosphere and the magnetosheath, for a current sheet thickness of 2 ion skin depths (as discussed below), and for $B_1 = 250$ nT and $B_2 = -161$ nT, Eq. (8) gives $E_X = 189$ mV/m, whereas the measured average value is 162 mV/m. For $M = 0.1$, Eq. (3) predicts $E_Y = 17$ mV/m, which compares with the 4 s averaged E_Y of 24 mV/m. The uncertainty in the average E_Y is the same order as the measured value because

(1) the temporal fluctuations of E_Y during different time intervals over which it may be averaged can change the result by a factor of 2.
(2) The uncertainty in E_Y associated with the rotation of the data into the minimum variance frame is similar to the magnitude of E_Y because E_X is an order-of-magnitude larger than E_Y.
(3) The translation of the data along the X-axis into the frame of the magnetopause changes E_Y by an amount comparable to its value, which has not been done for the data of Fig. 2 because the magnetopause speed over the spacecraft is not known.

For these reasons, E_Y cannot be used to test Eq. (3), and we shall use the measured E_X to test Eq. (8). The uncertainty in E_X does not depend on problems 2 and 3 above, but the selection of the averaging interval does affect the result. The −161 nT average of the last 30 s of data in Fig. 2(a) was used as the magnetosheath B_2 in the following analysis because this was its average value after the illustrated time interval. However, the uncertainty in this parameter can be typically ~25%, which must be remembered when evaluating the following statistical analyses.

Forty-eight reconnection events were collected during 2001–2003 and at other times of major magnetic storms when the magnetic local time at the spacecraft was between 0900 and 1500 and the magnetic latitude was less than 35°. E_X for each of these events is plotted versus Eq. (8) with $d = 1$ in panel (b) of Fig. 3. The 16 events having plasma outflow velocities >300 km/s are described in panel (a) of this figure. These 16 events are considered to be more reliable than the remaining 32 events because the spacecraft may have been closer to the diffusion region and active reconnection during each of them. The largest electric field event in Fig. 3 is the event shown in Fig. 2.

For Fig. 3(a), the correlation coefficient R^2, which is the fraction of the total squared error explained by Eq. (8), is a surprisingly large 0.90. This and the R^2-value of 0.84 in panel (b) strongly support the conclusion that the magnetic flux reconnection rate and the energy conversion rate depend on powers of the reconnection magnetic field.

The functional dependence of the electric field on the magnetic field and the plasma density has been studied by computing the correlation coefficients of the least-squares fits to different functions of B and n_0, as given in Table I. Examination of these R^2-values shows that

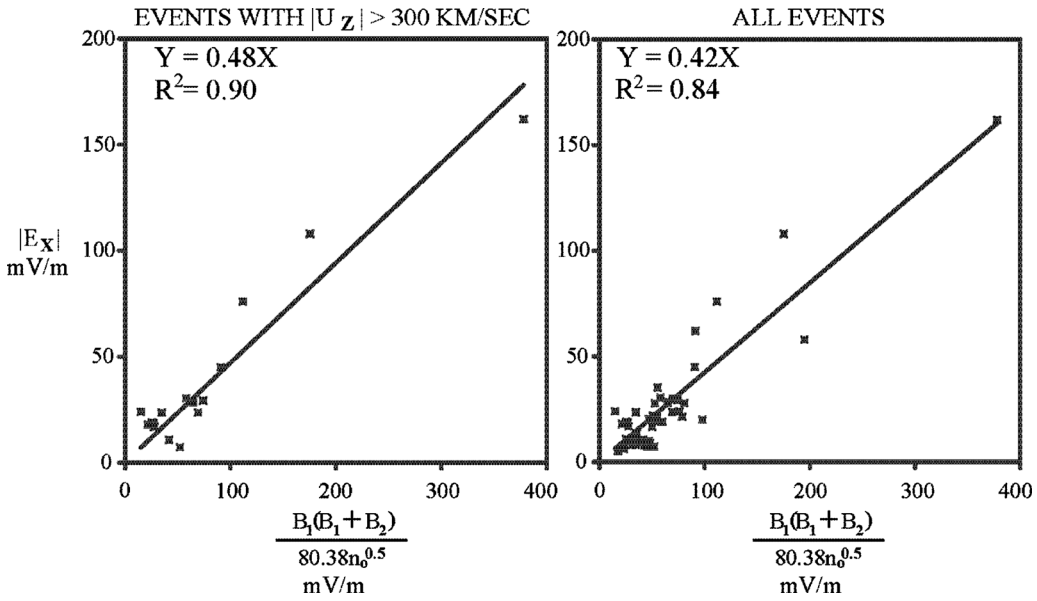

FIG. 3. Linear least-squares fits of E_X to Eq. (8) with d=1, measured at 48 subsolar magnetopause crossings in panel (b) and to the 16 of these crossings having a plasma outflow speed greater than 300 km/s in panel (a).

- the best overall fit to E_X is given by the functional form $B_1(B_1+B_2)/n_0^{0.5}$;
- the $B_1(B_1+B_2)$ dependence provides a better fit than does either $[B_1(B_1+B_2)]^{0.5}$ or $[B_1(B_1+B_2)]^{1.5}$ dependence; and
- including the plasma density provides better fits than not including it.

It is noted that the value of R^2 for 16 events and a functional dependence proportional to $[B_1(B_1+B_2)]^{0.5}$ is large relative to the other values. This is because B and n_0 roughly scale together, so a B dependence is not greatly different from a $B^2/n_0^{0.5}$ dependence.

The current sheet thickness found from the slope of the least-squares fit of Fig. 3(a) is about 2 ion skin depths. This result is consistent with other estimates[3] and adds validity to the entire procedure. The dependences of the measured and scaled electric fields have been compared with the magnitude of the measured guide magnetic field (which ranged from 0.1 to 1.1) and no relationship was found.

V. APPLICATION TO THE SOLAR SYSTEM

During its impulsive phase, a solar flare may release as much as 10^{25} J of energy in ~1000 s (10^{22} W). This phase is often followed by a gradual phase involving helmet streamers that have a reconnectionlike magnetic field geometry, from which $\sim 10^{23}$ J may be released. Surprisingly, as much as 50% of this energy ends in accelerated electrons.[15] It is often assumed that these 10^{20}–10^{22} W are released by reconnection in the solar corona. Assuming a magnetic field of 100 G and a plasma density of 10^8 cm^{-3} (each of which could be an order-of-magnitude different) at a reconnection site in the solar corona,[16] the energy release per unit area from Eq. (4a) is 10^7 W/m^2, which is a factor of 10^{11} greater than that at the terrestrial magnetopause. If the power of 10^7 W/m^2 is converted over an area of 20 000 $\times$ 20 000 km^2 (which is 10^6 proton skin depths by 10^6 proton skin depths or 0.01% of the solar surface area), the electromagnetic energy released by one reconnection event is sufficient to power solar flares and helmet streamers. The addition of multiple reconnection sites and the formation of islands that coalesce to release further energy can reduce the required area by a large factor.[17,18] The benefit of the scaling law is that the requirement on the area of the reconnection site or the multiple reconnection and island formation is diminished by a factor of $\sim 10^{10}$ from that required in the absence of the scaling.

TABLE I. R^2 for different functions of B and n_0.

	16 events	48 events
$[B_1(B_1+B_2)]^{0.5}$	0.83	0.59
$[B_1(B_1+B_2)]^{1.0}$	0.74	0.68
$[B_1(B_1+B_2)]^{1.5}$	0.40	0.36
$[B_1(B_1+B_2)]^{0.5}/n_0^{0.5}$	0.49	0.37
$[B_1(B_1+B_2)]^{1.0}/n_0^{0.5}$	0.90	0.84
$[B_1(B_1+B_2)]^{1.5}/n_0^{0.5}$	0.58	0.56

At the 9.5 solar radius perihelion of the Solar Probe Plus satellite, the convection electric field can be tens of V/m and the convective flow can be thousands of km/s. Instruments must be designed with these dynamic ranges in mind.

Messenger satellite observations of Mercury's magnetotail[19] have shown that marked increases of the tail field are probably caused by enhanced reconnection and that the magnetic energy content of the tail increased at a rate greater than five times that at similar events in the terrestrial magnetotail. Equation (3) states that the flux loading per unit time is proportional to $B_0^2/n_0^{0.5}$. Although the plasma density at Mercury was not measured, the fact that the observed magnetotail field at Mercury was greater than or equal to five times larger than that in the terrestrial magnetotail suggests that the Mercury tail observations were associated with en-

hanced flux reconnection on the dayside due to the larger solar magnetic field in its vicinity.

The role of magnetic field reconnection at Jupiter has been a topic of many discussions, with views ranging from reconnection producing an open magnetosphere to a viscous interaction along the magnetopause, which, in combination with the large internal magnetic field, internal plasma sources, and fast rotation, dictates the closed magnetospheric dynamics.[20] The uncertainties in the magnetic fields and densities at the subsolar Jovian magnetopause allow only a qualitative estimate of the electromagnetic energy conversion rate per unit area due to reconnection. For a reconnecting magnetic field of 1–2 nT and a plasma density of $\sim 1\ \mathrm{cm}^{-3}$, the energy conversion rate is more than 10 000 times smaller at Jupiter than at the terrestrial magnetopause. This supports the view that reconnection may be unimportant compared to other processes responsible for auroral activity on Jupiter, as has been noted.[21]

It has been shown that the intensity of Saturn's auroral emissions depends on solar wind pressure and internal processes,[21,22] so reconnection may not be important. This may be explained by the fact that the $B^3/n^{0.5}$ energy conversion rate factor is at least 15 000 times smaller for Saturn than for the Earth.

VI. APPLICATION TO HIGH ENERGY ASTROPHYSICS

Because astrophysical objects are observed to have maximum particle energies that depend on a power of the magnetic field[5] and because the acceleration mechanisms that produce them are not well understood,[4,23] it would be desirable to extrapolate the scaling laws of this paper to such objects. If the electric field scaling in such regimes is also proportional to the Alfvén speed (equal to the speed of light) times B, which is a scaling of energy conversion per unit area proportional to B^2, then a significant energy release from reconnection could be achieved in astrophysical objects.

ACKNOWLEDGMENTS

This work was supported by NASA, under Grant No. NNX09AE41G-1/11. The authors thank Professor Fran Bagenal, Dr. Hugh Hudson, and Professor Michael Shay for the helpful comments and information.

[1] V. M. Vasyliunas, Rev. Geophys. Space Phys. **13**, 303 (1975).
[2] F. S. Mozer and P. L. Pritchett, Phys. Today **63**(6), 34 (2010).
[3] E. G. Zweibel and M. Yamada, Annu. Rev. Astron. Astrophys. **47**, 291 (2009).
[4] P. P. Kronberg, S. A. Colgate, H. Li, and Q. W. Dufton, Astrophys. J. **604**, L77 (2004).
[5] A. M. Hillas, Annu. Rev. Astron. Astrophys. **22**, 425 (1984).
[6] M. Shay, J. F. Drake, and B. N. Rogers, J. Geophys. Res. **26**, 2163 (1999); J. Birn and M. Hesse, *ibid.* **106**, 3715 (2001).
[7] F. S. Mozer and A. Retinò, J. Geophys. Res. **112**, A10206 (2007).
[8] A. Vaivads, A. Retinò, and M. André, Space Sci. Rev. **122**, 19 (2006).
[9] M. A. Shay, J. F. Drake, and M. Swisdak, Phys. Plasmas **11**, 2199 (2004).
[10] P. A. Cassak and M. A. Shay, Phys. Plasmas **14**, 102114 (2007).
[11] P. A. Cassak and M. A. Shay, Geophys. Res. Lett. **35**, L19102 (2008).
[12] M. Hesse, J. Birn, and M. Kuznetsova, J. Geophys. Res. **106**, 3721 (2001); U. Becker, T. Neukrich, and K. Schindler, *ibid.* **106**, 3811 (2001).
[13] J. R. Sanny, R. L. McPherron, C. T. Russell, D. N. Baker, T. I. Pulkkinen, and A. Nishida, J. Geophys. Res. **99**, 5805 (1994).
[14] F. S. Mozer, V. Angelopoulos, J. Bonnell, K. H. Glassmeier, and J. P. Mcfadden, Geophys. Res. Lett. **35**, L17S04 (2008)
[15] R. P. Lin and H. S. Hudson, Sol. Phys. **17**, 412 (1971).
[16] D. J. Mullan, *Physics of the Sun: A First Course* (Chapman and Hall, London/CRC, Dordrecht, Netherlands, 2010).
[17] J. F. Drake, M. Swisdak, H. Che, and M. A. Shay, Nature (London) **443**, 553 (2006).
[18] M. Oka, T. D. Phan, S. Krucker, M. Fujimoto, and I. Shinohara, Astrophys. J. **714**, 915 (2010).
[19] J. A. Slavin, B. J. Anderson, D. N. Baker, M. Benna, S. A. Boardsen, G. Gloeckler, R. E. Gold, G. C. Ho, H. Korth, S. M. Krimigis, R. L. McNutt, Jr., L. R. Nittler, J. M. Raines, M. Sarantos, D. Schriver, S. C. Solomon, R. D. Starr, P. M. Trávníček, and T. H. Zurbuchen, Science **324**, 606 (2010).
[20] P. A. Delamere and F. Bagenal, J. Geophys. Res. **115**, A10201 (2010).
[21] J. T. Clarke, J. Nichols, J.-C. Gerard, D. Grodent, K. C. Hansen, W. Kurth, G. R. Gladstone, J. Duval, S. Wannawichian, E. Bunce, S. W. H. Cowley, F. Crary, M. Dougherty, L. Lamy, D. Mitchell, W. Pryor, K. Retherford, T. Stallard, B. Zieger, P. Zarka, and B. Cecconi, J. Geophys. Res. **114**, A05210 (2009).
[22] J. T. Clarke, J.-C. Gerard, D. Grodent, S. Wannawichian, J. Gustin, J. Connerney, F. Crary, M. Dougherty, W. Kurth, S. W. H. Coowley, E. J. Bunce, T. Hilll, and J. Kim, Nature (London) **433**, 717 (2005).
[23] C. A. Thompson and R. C. Duncan, Mon. Not. R. Astron. Soc. **275**, 255 (1995).